Regarding the perturbed operating process of DB propellant rocket motor at extreme initial grain temperatures

Doru SAFTA*,[1], Titica VASILE[1], Ioan ION[2]

*Corresponding author
*,[1]MTA - Military Technical Academy
B-dul George Coşbuc 81-83, Bucharest 050141, Romania
doru.safta@yahoo.com, vasiletitica@yahoo.com
[2]University "Eftimie Murgu"
Piata Traian Vuia 1-4, Reşiţa 320085, Romania
ioan.resita@yahoo.com

Abstract: Despite many decades of study, the combustion instability of several DB propellants is still of particular concern, especially at extreme grain temperature conditions of rocket motor operating. The purpose of the first part of the paper is to give an overview of our main experimental results on combustion instabilities and pressure oscillations in DB propellant segmented grain rocket motors (SPRM-01, large L/D ratio), working at extreme initial grain temperatures. Thus, we recorded some particular pressure-time traces with significant perturbed pressure signal that was FFT analysed. An updated mathematical model incorporating transient frequency-dependent combustion response, in conjunction with pressure-dependent burning, is applied to investigate and predict the DB propellant combustion instability phenomenon. The susceptibility of the tested motor SPRM-01 with DB propellant to get a perturbed working and to go unstable with pressure was evidenced and this risk has to be evaluated. In the last part of our paper we evaluated the influence of recorded perturbed thrust on the rocket behaviour on the trajectory. The study revealed that at firing-table initial conditions, this kind of perturbed motor operating may not lead to an unstable rocket flight, but the ballistic parameters would be influenced in an unacceptable manner.

Key Words: thermodynamics of rocket propulsion, steady and unsteady flows, unsteady combustion, ccombustion instability, pressure-coupled response function, flight dynamics

I. COMBUSTION INSTABILITIES AND PRESSURE OSCILLATIONS IN DB PROPELLANT ROCKET MOTORS WORKING AT EXTREME INITIAL GRAIN TEMPERATURES

I.1 INTRODUCTION

As a rocket in-flight is exposed to extreme temperatures, from 220K up-to 340K, it is very important to see how the solid propellant performs in these extreme temperature variations.

The first part of the paper is focused on the analyse of our main experimental results on combustion instabilities and pressure oscillations in the solid rocket motors (SPRM-01, large L/D ratio) with Double Base (DB) propellants. We took into account the main differences between DB propellants and their modern successor such as their homogeneous nature, very predictable and constant burn rate and smokeless exhaust products, which has made this type of propellants very tactically attractive for military applications. The DB solid propellant

motors usually used for small and medium tactical missiles are characterized by high pressure levels, short burning times and rather complex grain shapes.

The perturbed operating process especially at extreme initial grain temperatures is a potential problem in the development of any new solid rocket motor and it can occur even after the start of production. In our researches we recorded some particular pressure-time profiles at extreme ambient temperatures (233; 313) K with significant perturbed pressure signal that was FFT analysed.

The classical linearized theory of unsteady combustion of homogeneous propellants is based on the assumption of quasi-steady (QS) reaction zones in both the gas and condensed phases. This theory was developed on the basis of the flame modelling (FM) approach or of the phenomenological Zeldovich-Novozhilov (ZN) approach. The main difference between these two models is the source of the steady state burning information.

DB propellant thermocouple measurements have hinted the simple Arrhenius surface pyrolysis might be valid by suggesting a unique $r_b(T_s)$ relationship but have not been accurate enough to prove it [2, 8]. For all the effort that has gone into linear QS modelling (by either FM or ZN) the degree of quantitative success in predicting experimental results has been rather limited. The almost universal neglect of the effect of combustion product thermal radiation on the combustion response [8, 9, 12] is among the sources of error. Radiant flux is even today almost never adequately characterized in steady state burning rate measurements. Motors and strand burners can have very different radiant flux levels as can motors have different size.

As a result, parameters measured from strands (q_r near zero) have been commonly misapplied to solid rocket motors or T-burners to try to predict unsteady response, resulting in more confusion.

Another problem found [8, 13] in the early (particularly FM) literature is that the sensitivity parameters were assumed constant and the inherent dependence of these parameters on the independent variables T_i and p was ignored. Furthermore, the QS reaction zone assumption has not been adequately investigated.

In our paper the linearized QS theory is re-examined using a particular "flame model" for the condensed phase reaction zone as a high activation energy thermal decomposition model. An updated mathematical model incorporating transient frequency-dependent combustion response, in conjunction with pressure-dependent burning, is applied to investigate and predict the DB propellant combustion instability phenomenon. The model is used to predict T-burner data for uncatalyzed homogeneous DB propellants. The comparison is quite good using only reasonable, acceptable measured steady state burning parameters.

Final designs of solid rocket motors must be free of combustion instability and the motor performance characteristics must stay within specified acceptable limits.

I.2 ROCKET MOTOR PRESSURE MEASUREMENTS ON THE TEST STAND

Our experimental researches were guided to study the behaviour of DB solid propellants in the combustion process inside several rocket motors at extreme ambient temperatures. The motors were fired over the temperature range of 223 K to 323 K.

Among the many experiments on the test stands (static ground tests) at grain extreme initial temperatures, we recorded some particular pressure-time traces with perturbed pressure signal. These experimental pressure – time curves obtained with the same solid

rocket motor type SPRM-01, $((L/D)_{SRM} = 2117/122 = 17.35$, $(L/D)_{bc} = 1920/114 = 16.84$, $A_e/A_t = 3.84$, $(K_n)_i = (A_b)_i/A_t = 335.14)$ with DB-Propellant "DBP-01"(56% NC, 26.7% NG, 10.5% DNT, 3% EC, 3.8% miscellaneous; $\sigma_p = 0.00365$), pointed out the presence of significant combustion instabilities. Lower values of the temperature coefficient of the burning constant are favoured by inclusion of DNT in the propellant composition.
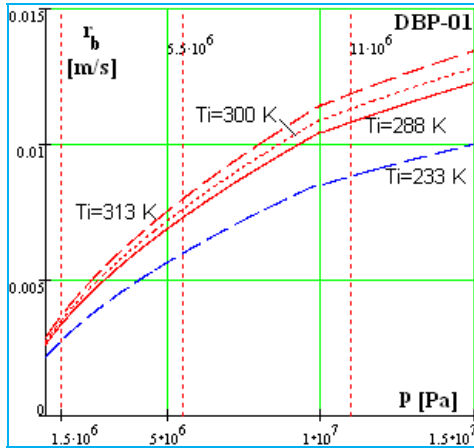

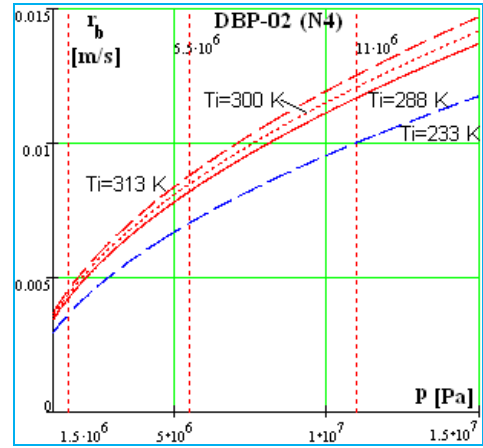Fig. 1 Burning rate variation $r_b(p)$ for DBP-01   Fig. 2 Burning rate variation $r_b(p)$ for DBP-02

Burning rate laws for two DB propellants types, DBP-01 and DBP-02 (similar with N-4, $\sigma_p = 0.0028$) [8, 13], at four different initial grain temperatures (233 K, 288 K, 300 K and 313 K), are shown in Fig. 1, 2. The burning rate experimental values were determined by means of the standard ballistic evaluation motor 32/ 16.
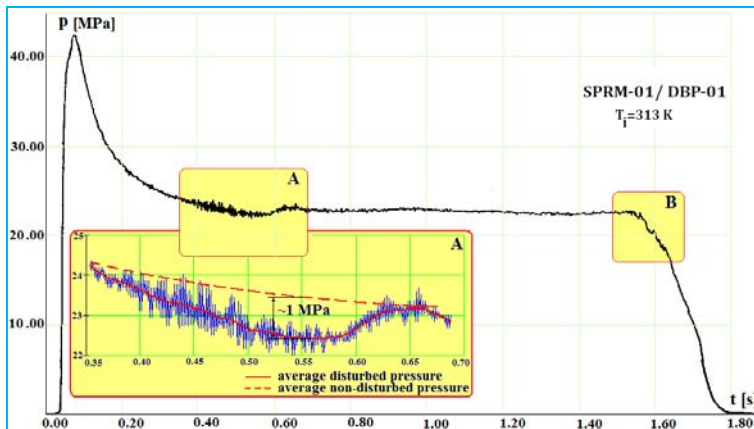

Fig. 3 Pressure – time history, at $T_i = 313K$, for SPRM - 01/ DBP-01

The experiments with cylindrically perforated grain using DBP-01, generally were reproducible as a result of careful manufacturing control and extended propellant curing time. Unstable combustion observed in the SPRM-01 was often characterized by not very high frequency chamber pressure oscillations and, sometimes accompanied by changes in the mean burning rate.

At extreme low initial temperatures pressure oscillations around the average signal with rather high amplitudes and low frequencies can appear (Fig. 4, 5). Lower frequency oscillations in a rocket motor may be associated with the pressure exponent of the propellant burning rate and the dimensions of the free volume of the motor chamber. Fig. 4 depicts a typical oscillatory combustion phenomenon which operates in the first half of the burning time, in two distinct zones being the result of the interaction between the acoustics of the cavity and the pyrolysis of the propellant.

We also have observed that in certain conditions rather high level frequency combustion instabilities can occur inducing an important variation of the average pressure evolution (Fig.5). The most disturbed time-pressure evolution (nonlinear instabilities) was recorded for smaller pressure values, corresponding of very low propellant initial temperature. The most intensive unstable burning at a real rocket motor as SPRM-01, with variable radial acceleration, occurred at initial grain temperature of 233 K (Fig. 5).

Many distinguished disturbed works were observed for DB propellant grains tested in standardized ballistic evaluation motors at initial grain temperatures greater than 300 K. We notice that combustion instabilities at high frequencies and small amplitudes were met especially at extreme positive ambient temperatures as in Fig. 3. At sufficiently high pressure levels, corresponding to higher initial grain temperatures, all firings were stable. When the pressure exceeds about 20 MPa, the oscillations of the burning rate start to grow. Reduction of the operating level could usually lead to mild combustion instability.

In the frequency range 100–1200 Hz, common for almost of all recorded SPRM-01 firings, the combustion instabilities were usually encountered in the axial modes of the rocket motor.
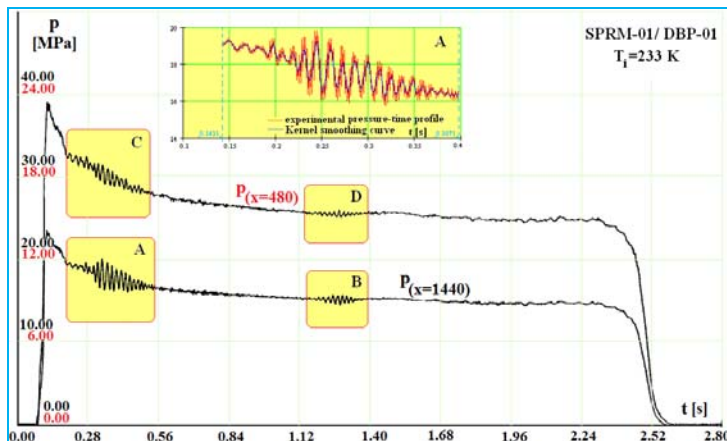

Fig. 4 Pressure – time history, at $T_i = 233K$, for SPRM-01/ DBP-01

No widely accepted theoretical model exists and the use of experimental data is required to predict the energy gains. To be able to predict the pressure coupled response it is necessary to determine the response/ admittance function of the propellant. The T-Burner is the industry standard device for more than 50 years to obtain the response function. The T-Burner is, however, labour intensive and expensive to maintain. A viable alternative is required in the tactical missile environment.

Our experimental researches concerning the combustion instability of DB propellants were done by using a T-burner device and also an adequate setup, built in our lab on the basis of the device developed by ONERA researchers (Fig. 6, 7, 8). This perturbed working

simulation device, in the frame of jet intermittent modulating techniques, can offer useful investigation opportunities [2, 5]. Although this device is not really a continuous pulsator, this method could be used to drive selected frequencies during an experiment and numerous pulses could be obtained in a single test.
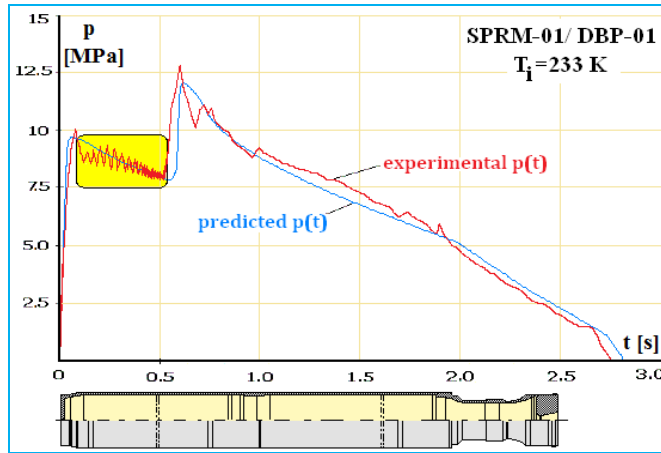

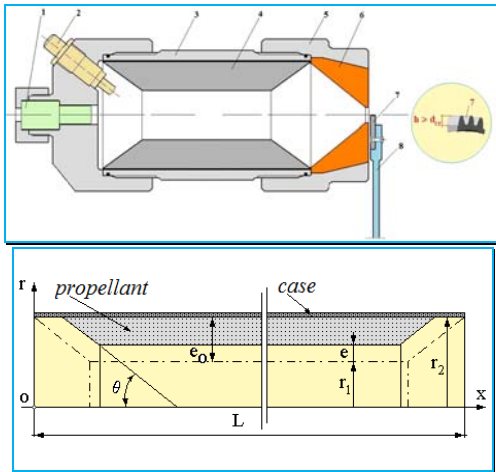Fig. 5 Pressure – time history, at $T_i = 233K$, SPRM-01/ DBP-01

Fig. 6 Sketch of subscale test motor with modulating device: 1 – dynamic quartz piezoelectric sensor, 2 – igniter,
3 – chamber wall, 4 – propellant grain,
5 – aft end cover, 6 – nozzle,
7 – modulating teeth, 8 – modulating wheel

Fig. 7 Schematic of propellant grain geometry

Fig. 8 Subscale test motor with variable length chamber

I.3 EVALUATION OF THE PROPELLANT COMBUSTION RESPONSE TO THE COUPLING PRESSURE

In our paper we will consider the *pressure coupled response*, as a response complex function for pressure fluctuations, which is the often referred parameter to describe the combustion instability characteristics of a solid rocket propellant. The nonlinear solid propellant response to a pressure perturbation produced close to the combustion surface can be obtained as an extension of the linear response derivation keeping the second order driving terms. Even these additional terms make the models more complicated, this nonlinear model can depict some effects, but the linear models can't describe them. Thus, a nonlinear model can predict

the time evolution of a system and offer response functions depending on amplitude and frequency.

In order to make analysis easier to implement, and amenable to solution, many simplifying assumptions are considered in our presentation, but the essential features of the combustion – flow process are retained in our study model.

We assume the solid and gas phases are Homogeneous (H) and the combustion is One-Dimensional (OD). The conversion of condensed material to the gas phase is done at an infinitesimally thin interface and the flame is anchored on it. The model is based on a non-reacting condensed phase and on a Quasi-Steady (QS) behaviour of all processes *except unsteady conductive heat transfer in the condensed phase*. The pyrolysis surface phenomenon is described by the Arrhenius law. This modelling frame is known as the *(QSHOD) model* [2].

We have chosen a reference system with origin ($x = 0$) fixed in space to the average position of the interface. The cold un-reacted solid propellant progresses inward from the left side with a constant velocity equal with the steady state burning rate, $\bar{r}_b$ and the combustion surface oscillates around the origin during the combustion instability process, Fig. 9.
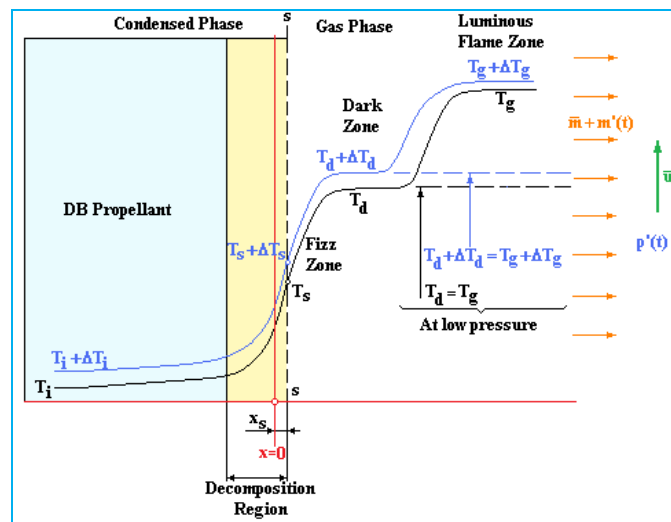

Fig. 9 Combustion wave structure of a DB propellant at different initial temperatures
and at high and low-pressures

The analysis of available experimental data for rocket propellants provided new arguments in the favour of the concept that the condensed phase is the locus of the *burning rate control zone* at the operating pressure range of the solid rocket motors [1, 2]. Our analysis involves only three steps: solution for the temperature field in the solid phase, solution for the temperature field in the gas phase and matching the two solutions at the interface level. Thus, we will give, first of all, a solution for the solid phase. The energy equation for the solid phase assumed to have uniform and constant properties, is

$$\lambda_p \frac{\partial^2 T}{\partial x^2} - \overline{m} c \frac{\partial T}{\partial x} - \rho_p c \frac{\partial T}{\partial t} = -\dot{Q}_d, \tag{1}$$

where $(\bar{})$ means time-averaged value, $(\ )_p$ denotes propellant, c is the specific heat of the solid phase, $\overline{m} = \rho_p \bar{r}_b$ is the average mass flux in the reference system and $\dot{Q}_d$ is the rate at

which energy is released per unit volume due to decomposition of the solid (is determined by chemical reactions in a thin layer of propellant surface; $\dot{Q}_d > 0$ for exothermic decomposition). We can assume [2] $\dot{Q}_d = 0$ and the solution of the eq. (1) rewritten using the propellant thermal diffusivity α_p, eq. (2), can take for harmonic motions the form:

$$\alpha_p \cdot \frac{\partial^2 T}{\partial x^2} = \frac{\partial T}{\partial t} + r_b \cdot \frac{\partial T}{\partial x}, \qquad \alpha_p = \frac{\lambda_p}{\rho_p c}, \tag{2}$$

$$T(x,t) = \underbrace{\overline{T}(x)}_{steady} + \underbrace{T'(x,t)}_{time-dependent} = \overline{T}(x) + \underbrace{\widetilde{T}(x) \cdot e^{i\omega t}}_{harmonic\ motions}, \quad |T'| \ll \overline{T}. \tag{3}$$

Due to the choice of reference system, the amplitude $\widetilde{T}(x)$ in (3) is the fluctuation of temperature at the average position of the interface ($x = 0$).

On the basis of the boundary conditions:

$$\overline{T} = T_i, \ T' = 0 \ \text{ when } x \to -\infty; \quad \overline{T} = \overline{T}_s, \ T' = T'_{0-} \ \text{ when } x = 0, \tag{4}$$

the solution takes the form:

$$T = T_i + (\overline{T}_s - T_i) \cdot e^{r_b x / \alpha_p} + T'_{0-} \cdot e^{\lambda r_b x / \alpha_p} \cdot e^{i\omega t}, \tag{5}$$

where the eigenvalue λ is depending on the dimensionless frequency $\Omega = \omega \alpha_p / r_b^2$:

$$\lambda(\lambda - 1) = i\Omega \quad \Rightarrow \quad \lambda_r = \frac{1}{2}\left\{ 1 + \frac{1}{\sqrt{2}}[(1 + 16\Omega^2)^{1/2} + 1]^{1/2} \right\}. \tag{6}$$

The required results for the upstream side of the interface cannot be completed until the interfacial region is analyzed. The energy balances at the interface level for steady and for unsteady conditions are:

$$\lambda_g \left(\frac{d\overline{T}}{dx} \right)_{s+} = \lambda_p \left(\frac{d\overline{T}}{dx} \right)_{s-} - \overline{m}_s \overline{Q}_s, \tag{7}$$

$$\lambda_g \left(\frac{dT'}{dx} \right)_{s+} = \lambda_p \left(\frac{dT'}{dx} \right)_{s-} - m'_s \overline{Q}_s - \overline{m}_s Q'_s - m'_s Q'_s, \tag{8}$$

where Q_s is over-all heat per unit mass liberated at the combustion surface.

On the basis of the temperature profile, eq. (5) and using

$$T'_{s-} = T'_{0-} + \left(\frac{d\overline{T}}{dx} \right)_{0-} x_s, \quad \dot{x}_s = -k\omega x_s, \tag{9}$$

and assuming no perturbation of Q_s, the right side member of eq.(8) can be written:

$$\lambda_p \left(\frac{dT'}{dx} \right)_{s-} = \overline{m}_s c \overline{T}_s \left[\lambda \frac{T'_s}{T_s} + \frac{1}{\lambda}\left(1 - \frac{T_i}{T_s} \right) \frac{m'_s}{\overline{m}_s} \right], \tag{10}$$

where: x_s is the transient position of the combustion surface with respect to the fix origin, T'_{0-} is the temperature fluctuation on the solid side of the origin, T'_{s-} the temperature fluctuation on the solid side of combustion surface and k a mode number.

For the left side member of eq. (8) that describes the quasi-steady response of the gas phase we can develop until the second order the energy balance equation of steady burning

$$\lambda_g \left(\frac{dT}{dx} \right)_{s+} = m_s \left[c(T_s - T_i) - Q_s \right], \tag{11}$$

and one can obtain:

$$\lambda_g \left(\frac{dT'}{dx} \right)_{s+} = \overline{m}_s c \overline{T}_s \left(1 - \frac{T_i}{\overline{T}_s} \right) \left[1 - \frac{\overline{Q}_s}{c(\overline{T}_s - T_i)} \right] \frac{m'_s}{\overline{m}_s} + \overline{m}_s c \overline{T}_s \frac{T'_s}{\overline{T}_s} + \overline{m}_s c \overline{T}_s \frac{m'_s}{\overline{m}_s} \frac{T'_s}{\overline{T}_s}. \tag{12}$$

Usually, an Arrhenius exponential law has been assumed for the conversion of solid to gas, giving the total surface mass flux:

$$m_s = B_s p^{n_s} e^{-E_s / \Re T_s} \tag{13}$$

This equation basically relates the surface temperature on the mass flux at the combustion surface and the frequency factor, B_s pressure power, n_s and activation energy, E_s are in most cases unknown functions.

Perturbing the eq. (13) and keeping the second order terms one can write:

$$\frac{m'_s}{\overline{m}_s} = n_s \frac{p'}{\overline{p}} + \frac{n_s(n_s - 1)}{2} \left(\frac{p'}{\overline{p}} \right)^2 + E \frac{T'_s}{\overline{T}_s} + n_s E \frac{p'}{\overline{p}} \frac{T'_s}{\overline{T}_s} + \left(\frac{E^2}{2} - E \right) \left(\frac{T'_s}{\overline{T}_s} \right)^2, \tag{14}$$

where $E = E_s / \Re \overline{T}_s$ is the dimensionless activation energy for the surface reaction.

The (14) is a second-degree equation in $T'_s / \overline{T}_s$ and a positive solution can be written as:

$$\frac{T'_s}{\overline{T}_s} = \frac{1}{E - 2} \frac{1}{2} n_s^2 \left(\frac{p'}{\overline{p}} \right)^2 + \frac{1}{E - 2} \left(1 - \frac{2}{E} \right) \left[\frac{m'_s}{\overline{m}_s} - n_s \frac{p'}{\overline{p}} - \frac{n_s(n_s - 1)}{2} \left(\frac{p'}{\overline{p}} \right)^2 \right] - $$
$$- \frac{1}{2} \frac{1}{E - 2} \left[\left(1 - \frac{2}{E} \right)^2 \left(\frac{m'_s}{\overline{m}_s} \right)^2 + \left(1 - \frac{2}{E} \right) \frac{4}{E} n_s \frac{m'_s}{\overline{m}_s} \frac{p'}{\overline{p}} + \left(\frac{2n_s}{E} \right)^2 \left(\frac{p'}{\overline{p}} \right)^2 \right]. \tag{15}$$

Taking into account eqs. (8), (10), (12) one gets the expression:

$$\frac{A}{E} (1 - H) \frac{m'_s}{\overline{m}_s} + \frac{T'_s}{\overline{T}_s} + \frac{m'_s}{\overline{m}_s} \frac{T'_s}{\overline{T}_s} = \left[\lambda \frac{T'_s}{\overline{T}_s} + \frac{1}{\lambda} \left(1 - \frac{T_i}{\overline{T}_s} \right) \frac{m'_s}{\overline{m}_s} \right] - \frac{AH}{E} \frac{m'_s}{\overline{m}_s}, \tag{16}$$

where the last term that defines the heat generation at the combustion surface will be transformed using:

$$\frac{m'_s}{\overline{m}_s} = n \frac{p'}{\overline{p}} + \frac{n(n - 1)}{2} \left(\frac{p'}{\overline{p}} \right)^2, \tag{17}$$

which supposes that the instantaneous burning rate during the acoustic oscillations governs the heat instantaneous emission at the combustion surface.

The A and H parameters of eq. 16 are given by:

$$A = \left(1 - \frac{T_i}{\overline{T}_s} \right) \cdot E, \quad H = \frac{\overline{Q}_s}{c(\overline{T}_s - T_i)}, \tag{18}$$

where A contains the activation energy associated with surface pyrolysis temperature and H is dependent only on the propellant solid phase characteristics.

A and H are often practically used as floating constants to be adjusted to fit experimental data; however, they do have a theoretical basis.

By adequate transformations of the eqs.(15), (16) and (17) one can write the pressure coupled response for the linear case:

$$R_b^\ell = \frac{m_s' / \overline{m}_s}{p' / \overline{p}} = \frac{nAH + (\lambda - 1)n_s}{\lambda + A/\lambda - (A+1) + AH}, \tag{19}$$

and for non-linear case:

$$R_b^{n\ell} = R_b^\ell + \left[C_1 \left(R_b^\ell \right)^2 + C_2 R_b^\ell + C_3 \right] \cdot \frac{p'}{\overline{p}}, \tag{20}$$

where the coefficient expressions are:

$$C_1 = \left[(\lambda - 1)\frac{E-2}{2E} + 1 \right] \cdot \left[\lambda + A/\lambda - (A+1) + AH \right]^{-1}, \ C_2 = \frac{n-1}{2},$$

$$C_3 = \left\{ \left[(\lambda - 1)\frac{2}{E} - 1 \right] n_s n + (\lambda - 1) \left[-\frac{E}{E-2}\frac{n_s^2}{2} + \frac{n_s(n_s - 1)}{2} + \frac{2n_s^2}{E(E-2)} \right] \right\} \cdot \tag{21}$$

$$\cdot \left[\lambda + A/\lambda - (A+1) + AH \right]^{-1}.$$

I.4 THE INFLUENCE OF THE INITIAL GRAIN TEMPERATURE ON THE DB PROPELLANT COMBUSTION NONLINEAR RESPONSE

On the basis of the mathematical model presented in I.3 we have first of all explored how the nonlinear pressure coupled response function behaves when the parameters $T_s, E_s/\mathfrak{R}, Q_s, n_s$ take significant values in their operating ranges for DB solid rocket propellants.

The effect of the pressure perturbation level on the propellant response is considered by the factor $p'/\overline{p}$ of the non-linear response function (20).

The R_p^{nl}/n and R_p^{nl}/R_p^l ratios were analysed with respect to the dimensionless frequency Ω for a pressure perturbation ratio $p'/\overline{p} = 0.1$ and $n_s = 0$, Fig. 10-15.

One may observe the stabilisation influence of the propellant non-linear response, R_p^{nl} for the low and high dimensionless frequency values (Fig. 11, 13 and 15). Some useful results are shown in Fig. 16 and 17, for none zero n_s values.

The effect of none zero n_s values to combustion instability, for the high dimensionless frequency domain, can be noticed.

Taking into account the main goal of our researches, we have investigated the behaviour of DBP-01, at the extreme initial temperatures of 233 K and 313 K, for a perturbation level $p'/\overline{p} = 0.1$, Fig. 18.

The average burning chamber pressures correspond to the SPRM-01 operating process at the mentioned grain initial temperatures.
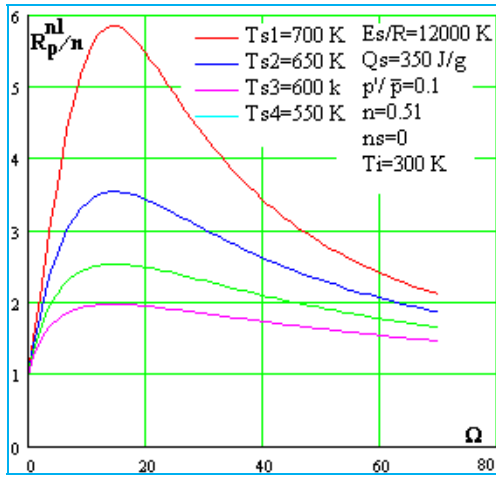
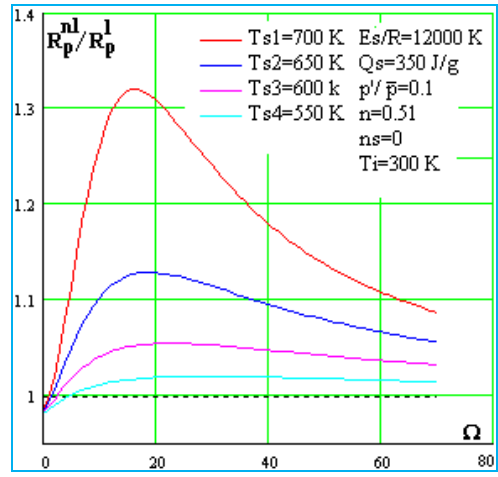Fig. 10 The influence of T_S on the R_p^{nl} / n ratio

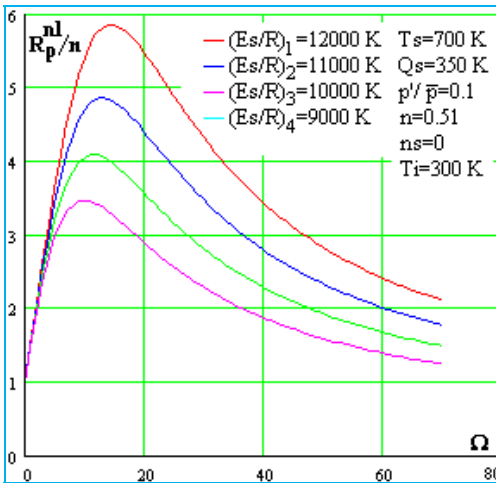Fig. 11 The influence of T_S on the R_p^{nl} / R_p^l ratio

Fig. 12 The influence of E_S / R on the R_p^{nl} / n ratio
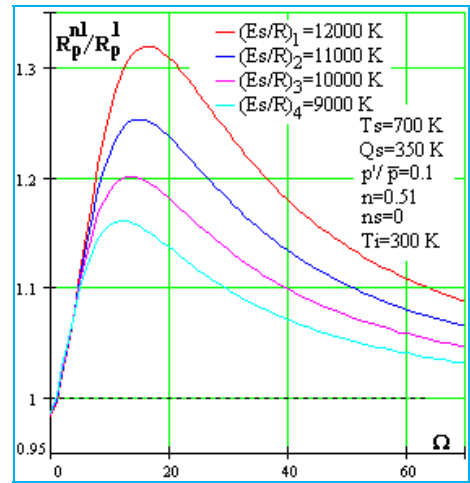

Fig. 13 The influence of E_S / R on the R_p^{nl} / R_p^l ratio
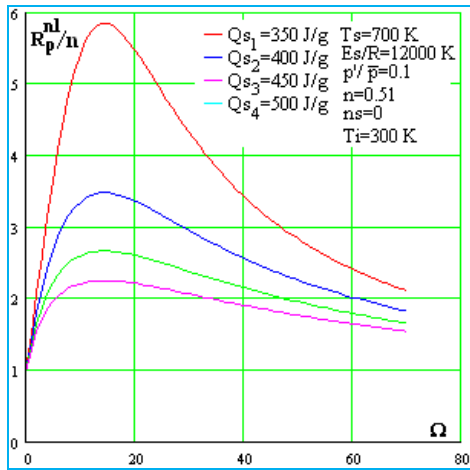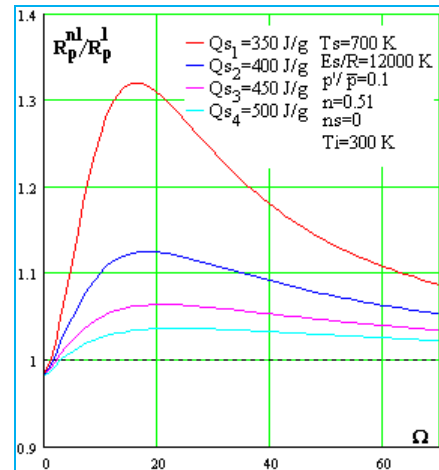

Fig. 14 The influence of Q_S on the R_p^{nl} / n ratio

Fig. 15 The influence of Q_S on the R_p^{nl} / R_p^l ratio

One can observe, analysing the diagram (Fig.18) concerning the influence $T_i \rightarrow R_p^{nl} / n$ that the most dangerous cases for the motor operating process appear at very low initial temperatures. This remark is in agreement with our experimental researches using SPRM-01 with DBP-01 at 233 K. Fig.19 depicts the variation of the DBP-01 non-linear response function depending on dimensionless frequency Ω, for different perturbation levels $(p' / \overline{p} = 0; 0.1; 0.3)$. Thus, the very low temperatures (233 K) coupled with a greater pressure perturbation level could affect the operating process by an intense combustion instability.
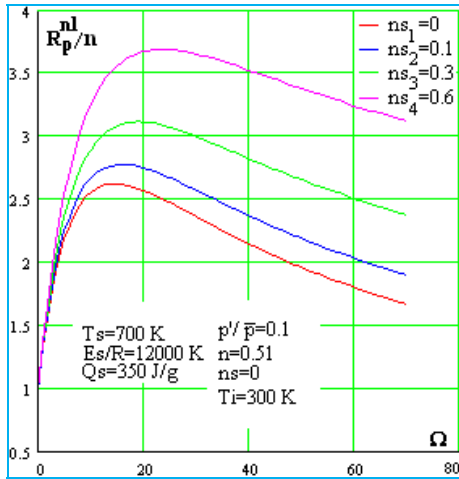

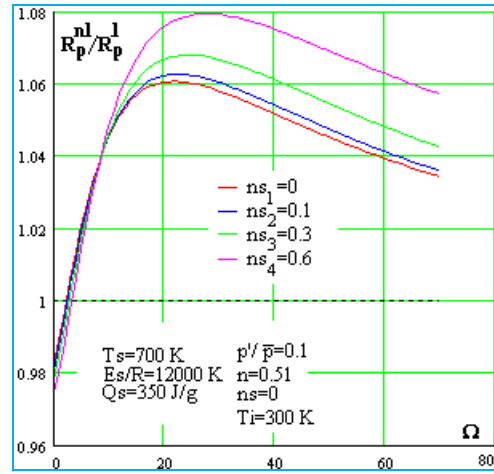Fig. 16 The influence of n_s on the R_p^{nl} / n ratio

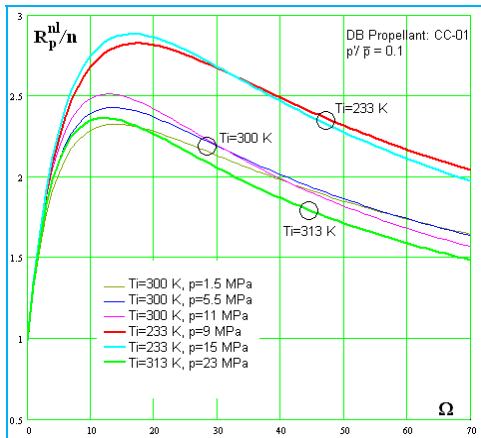Fig. 17 The influence of n_s on the R_p^{nl} / R_p^l ratio

Fig. 18 The influence of grain initial temperature on the R_p^{nl} / n ratio
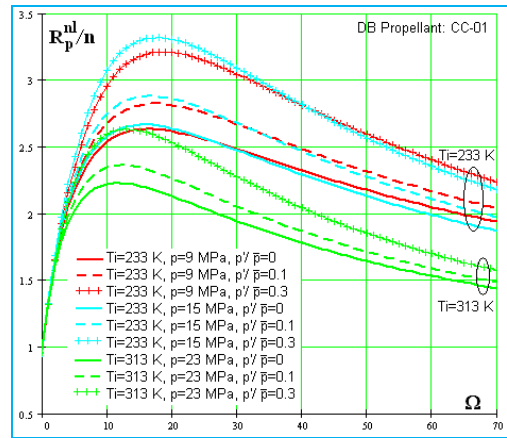

Fig. 19 The influence of pressure perturbation level on the R_p^{nl} / n ratio

II. THE INFLUENCE OF THE PERTURBED OPERATING PROCESS ON THE ROCKET FLIGHT

The change in the pressure/ thrust - time profile causes significant changes in the flight path, and at times this can lead to failure of the mission. For this reason, in the last part of our research we evaluated the rocket engine working influence over the rocket flight parameters.

The study of the rocket behaviour on the trajectory is developed in a first stage, on the basis of the mathematical model of *rocket longitudinal movement in a resistant environment* [15]. The case of the rocket flight with aerodynamical stability is considered. The rocket, like study object, is assumed with an axial symmetry configuration.

The longitudinal movement equations of the rocket under the action of the thrust, weight, drag, lift, taking into account the principal aerodynamic moment, the gas damping moment and the moment provided by the thrust gasdynamical asymmetry, using intrinsic coordinates, may be easily written as in [15]. This system, with given boundary conditions, can be numeric integrated in order to calculate the variations in time of the incidence and the others flight parameters along the trajectory.

The aerodynamic coefficients variations for a study rocket, $D_R = 127mm$, of static stable configuration (the mass and aerodynamical characteristics [15]), which were computed using methods in agreement with the experimental data, are shown in Fig.20-22.
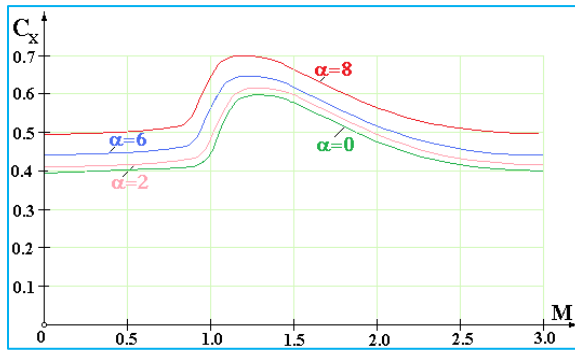

Fig. 20 $C_x(M)$ depending on the incidence α values

Some significant results, in a graphic form, of our numerical applications are presented in Fig. 23-26, for two distinct cases - the normal working and the unstable operating process of SPRM-01/ DBP-01, at 233 K (case presented in Fig.5). Thus, the ballistic parameters: rocket velocity (v), the rocket coordinates (x, y) on the powered trajectory period and the rocket range (X) were evaluated in normal and perturbed conditions (Fig. 23, 26).
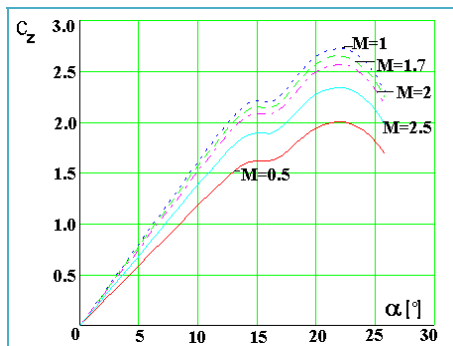

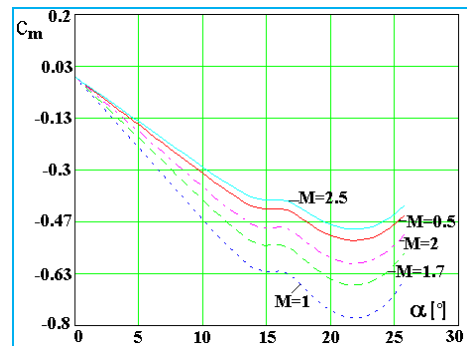Fig. 21 $C_z(\alpha)$ for different Mach number values

Fig. 22 $C_m(\alpha)$ depending on the Mach

We have preferred to get this ballistic analyse for different values of initial elevation angle θ_0 in order to obtain more useful and significant ballistic data. The ballistic parameters variation is affected by this kind of unstable engine working, at different elevation angles, even the rocket behaviour on the trajectory is acceptable. In this stage, our study included

also the investigation of the influence of the perturbed thrust at 233K on the flight dynamics parameters: α, ω, φ and θ, (Fig. 24, 25). Thus, with an unguided rocket projectile at firing-table initial conditions a stable flight is obtained (Fig. 24), in resistant environment, even for the unstable engine operating process. One can observe that the variation of incidence angle and the pitching oscillations present a fast damping.
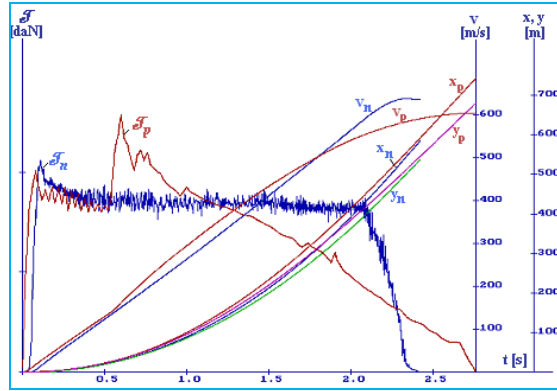

Fig. 23 The influence of the SPRM-01 perturbed thrust on the ballistic parameters (v, x, y)

Fig. 24 The influence of the SPRM-01 perturbed operating process on the flight dynamics parameters α, ω, φ and θ
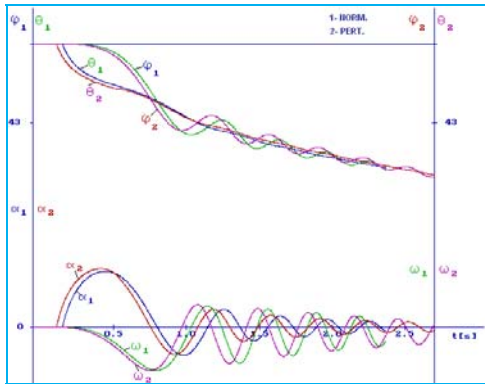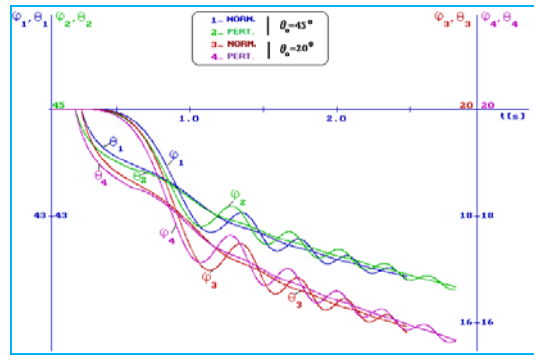

Fig. 25 The influence of the SPRM-01 perturbed operating process on the flight dynamics parameters φ and θ for $\theta_0 = 45^{\mathrm{o}}; 20^{\mathrm{o}}$
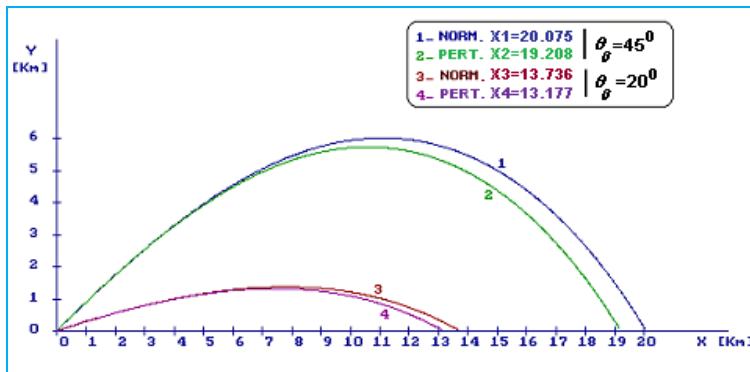

Fig. 26 The influence of the SPRM-01 perturbed operating process on the rocket range for $\theta_0 = 45^{\mathrm{o}}; 20^{\mathrm{o}}$

CONCLUSIONS

Much more disturbed time-pressure profiles with linear or non-linear instabilities were recorded at very low initial temperatures corresponding of smaller pressure values (Fig. 4, 5). We can outline rather low frequency of the average pressure oscillations that have distinct amplitudes in the two combustion instability zones that appeared at 233K during one static test (experimental perturbed pressure – time profile and Kernel smoothing curve at 233K in the A detail window of Fig. 4). The most intensive perturbed and unstable combustion at the real rocket motor SPRM-01, with variable radial acceleration, occurred at the same initial grain temperature of 233 K (Fig. 5 with detail window of perturbed pressure signal).

We have also noticed that combustion instabilities at high frequencies and small amplitudes were met especially at extreme positive ambient temperatures. The pressure-time history in our study case at 313K presents also a rather significant variation of the average chamber pressure of about 1MPa in the perturbed zone (perturbed pressure signal, average perturbed and non-perturbed pressure at 313K in the A detail frame of Fig. 3). When the pressure exceeds about 20 MPa, the oscillations of the burning rate start to grow. At sufficiently high pressure levels, corresponding to higher initial grain temperatures, all experimental static test firings were stable.

Prediction of the level of combustion instability requires in essence a non-linear approach. The nonlinear solid propellant response to a pressure perturbation produced close to the combustion surface was obtained as an extension of the linear response derivation keeping the second order driving terms (eqs. 19-24).

A parametric study of the theoretical results as well as comparisons with existing experimental data and numerical results are carried out. On the basis of an improved mathematical model we have explored how the nonlinear pressure coupled response function (eq. 20) behaves when the parameters $T_s, E_s/\Re, Q_s, n_s$ take significant values in their operating ranges for DB solid rocket propellants (Fig. 10-17). The diagram (Fig. 18) of the influence of grain initial temperature on the R_p^{nl}/n ratio depicts that the most dangerous cases for the motor operating process appear at very low initial temperatures. This remark is in agreement with our experimental researches using SPRM-01 with DBP-01 at 233 K.

The obtained propellant response function (eq. 20), by the factor $p'/\overline{p}$ take into account the effect of the pressure perturbation level on the propellant unsteady combustion. Very low temperatures coupled with a greater pressure perturbation level could affect the operating process by an intense combustion instability (Fig. 19).

Considerable data exists suggesting that the response functions for many solid propellants tend to have higher values, in some ranges of frequencies, than predicted by the conventional QSHOD theory. It is a familiar idea that such behaviour is associated with dynamical processes possessing characteristic times shorter than that of the thermal wave in the condensed phase. The QSHOD theory, and most of its variants, contains only the dynamics of that process, which normally has a characteristic frequency in the range of a few hundred hertz (Fig. 3-5, for our case studies).

Two different response mechanisms can be studied depending on the frequency range. In agreement with the well known quasi-steady theory, the low frequency response is mainly controlled by the thermal relaxation in the solid phase and is triggered through the pressure dependence of the pre-factors in the pyrolysis and burning laws. At high frequencies, the gas temperature fluctuations associated with pressure oscillations may introduce a new response mechanism of the burning rate independent of the pressure exponents. This response

mechanism involves the structure of the gaseous flame. The resulting vibratory instability may be stronger than the low frequency one.

Smaller ratios between the free initial volume of burning chamber and the nozzle critic area ($L^* < 150$), coupled with the very low grain initial temperatures (for example 233 K) can be very favourable for the appearance of a violent combustion instability zone (Fig. 5, for DBP-01). This kind of oscillations with not very high frequencies can induce an important deviation of the average pressure signal, as in our case study (more than 30%). This significant unstable motor working was conveniently simulated using our ballistic study model (Fig. 23, 26). Even in the case of a perturbed motor working, at firing-table initial conditions or at grain extreme initial temperatures, the rocket flight could be stable.

The ballistic parameters variation could be greatly influenced by the perturbed or unstable engine working, at different elevation angles, even when the rocket behaviour on the trajectory is acceptable (Fig. 26). Our researches pointed out also the presence of a trajectory initial critical period, its duration in our study case being smaller than the pitching oscillations period. An important conclusion for the rocket engine designers is that the propellant burning time must be longer than this initial critical period [15]. In practice, obviously, it is important to study the rocket movement at over limit and over critic incidences, in order to estimate the flight correctness at great incidence values, caused by different disturbances – especially at very low temperatures – and to establish the firing rockets safety areas.

Lack of accuracy of certain input data, especially for the condensed phases should be taken into account. The well known difficulty to improve the knowledge of combustion instability phenomenon is linked to the nearly impossibility to carry out detailed measurements inside an actual motor, even at a low scale and for a non-metallized propellant. However, some validations have been made by using a special small scale model with a dedicated instrumentation and the results are rather promising.

Research towards predicting and quantifying undesirable axial combustion instability symptoms necessitates a comprehensive numerical model for internal ballistic simulation under dynamic flow and combustion conditions. The study model of the present paper was included in the mathematical model of a complex simulation computer program of solid rocket motors disturbed working, which operates with a large termogasdynamical and engine construction data basis. This is also a benefit of using an indirect evaluation method of coupled pressure propellant response function.

NOMENCLATURE

A, H – parameters appearing in response function, eqs. (18);

c – specific heat of solid phase;

E_s – activation energy of surface pyrolysis reaction;

E – dimensionless activation energy of surface decomposition;

f – frequency of pressure oscillations;

$\bar{m}$ – average mass flux;

n – burning rate pressure exponent;

n_s – pressure power in eq.(13);

p – pressure;

Q_s – condensed phase heat release;

$\bar{r}_b$ – steady state propellant burning rate;

R_p^{ℓ} , $R_p^{n\ell}$ – propellant linear and non-linear response to the pressure coupling;

T_i – initial propellant temperature;

T_s – temperature of burning surface;

$\widetilde{T}$ – amplitude of temperature oscillation;

v – rocket velocity;

$\mathcal{T}$ – rocket motor thrust;

α – flight incidence angle;

α_p – propellant thermal diffusivity;

φ – pitch angle;

λ_p, λ_g – propellant and gas phase thermal conductivity;

θ – elevation angle;

σ_p – sensitivity of steady-state burning to bulk temperature;

ω – pulsation of pressure oscillations or pitching angular velocity of the missile;

Ω – dimensionless frequency of oscillations;

$\overline{(\ )}, (\ )'$ – time-averaged and fluctuation of a certain parameter;

$(\ )_s, (\ )_d, (\ )_g$ – denotes burning surface, dark zone and flame zone;

$(\ )_p$ – denotes propellant or a perturbed ballistic parameter.

REFERENCES

[1] F. S. Blomshield, *Lessons Learned In Solid Rocket Combustion Instability*, American Institute of Aeronautics and Astronautics, Missile Sciences Conference, Monterey, California, November 2006.
[2] F. E. C. Culick, *Combustion Instabilities in Solid Rocket Motors*, Notes for two lectures of special course "Internal Aerodynamics in Solid Rocket Propellant", von Karman Institute, 2002.
[3] G. M. Gadiot, A. Gany, Modelisation de l'instabilite due au couplage non lineaire par pression dans un moteur fuse a propergol solide, *La Recherché Aerospatiale*, No. 5, 23-37, 1988.
[4] P. Kuentzmann, A. Laverdant, Détermination expérimentale de la réponse d'un propergol solide aux oscillations de pression de haute fréquence, *La Recherche Aérospatiale*, 1984.
[5] D. Safta, T. Vasile, I. Ion, Regarding the Influence of High Frequency Combustion Instabilities on Operation of Solid Rocket Motors, *Problems of Mechatronics, Armament, Aviation, Safety Engineering*, Nr 1(3), ISSN 2081 5891, Military University of Technology, Warsaw, Poland, 2011.
[6] J. C. Traineau, M. Prevost, P. Tarrin, Experimental low and medium frequency determination of solid propellants pressure-coupled response function, *AIAA 94-3043*.
[7] N. S. Cohen, Response Function Theories That Account for Size Distribution Effects-A Review, AIAA Journal, Vol. 19, No. 7, ISSN: 0001-1452, E-ISSN: 1533-385X July 1981.
[8] M. Q. Brewster, S. F. Son, Quasi-steady Combustion Modeling of Homogeneous Solid Propellants, *Combustion and Flame 103*: 11-26, Elsevier, ISSN: 0010-2180, 1995.
[9] S. F. Son, M. Q. Brewster, Unsteady Combustion of Homogeneous Energetic Solids Using the Laser-Recoil Method, *Combustion and Flame 100*: 283-291, Elsevier, ISSN: 0010-2180, 1995.
[10] F.E.C. Culick, *A Review of Calculations forUnsteady Burning of a Solid Propellant*, ICRPG/ AIAA 2 nd Solid Propulsion Conference, Anaheim, Calif., June 6-8, 1968.
[11] D. R. Greatrix, Transient Burning Rate Model for Solid Rocket Motor Internal Ballistics Simulations, *International Journal of Aerospace Engineering*, Vol. 2008, ID 826070, ISSN: 1687-5966 (Print), ISSN: 1687-5974 (Online).
[12] V. E. Zarko, V. N. Simonenko, A. B. Kiskin, Study of Solid Propellant Combustion under External Radiation, *Defence Science Journal*, Vol. 42, No. 3, 183-189, ISSN: 0011-748X (Print), 0976-464X (Online), July 1992.
[13] N. Kubota, T. J. Ohlemiller, L. H. Caveny, M. Summerfield, *The Mechanism of Super-Rate Burning of Catalyzed Double Base Propellants*, Aerospace and Mechanical Sciences Report, Princeton University, 1973.
[14] R. S. de Boer, H. F. R. Schoyer, *Results of L* Instability Experiments with Double Base Rocket Propellants*, Delft University of Technology, Report, October, 1976.
[15] D. SAFTA, *Propulsion Thermodynamics and Fly Dynamics Elements*, Military Technical Academy, Bucharest, 2004.